Karlsruhe Institute of Technology

Calculation of Synthetic Energy Carrier Production Costs with high Temporal and Geographical Resolution

Uwe Langenmayr, Manuel Ruppert

No. 72 | SEPTEMBER 2023

WORKING PAPER SERIES IN PRODUCTION AND ENERGY

Calculation of Synthetic Energy Carrier Production Costs with high Temporal and Geographical Resolution

Uwe Langenmayr, Manuel Ruppert

Chair of Energy Economics, Institute for Industrial Production (IIP) at Karlsruhe Institute of Technology (KIT)
Hertzstraße 16., Building 06.33, 76187 Karlsruhe
Tel.: +49 721 608-44685
Mail: uwe.langenmayr@kit.edu

While the decarbonization of the electricity sector is proceeding globally with the ongoing increase of wind and solar generation, reducing the carbon footprint of other sectors such as industry, transportation, and agriculture proves more challenging. One reason is the challenge of electrifying processes in these sectors. Here, power-to-X applications can support the transformation of these sectors by replacing conventional energy carriers with synthetic energy carriers from renewable sources.

In this work, an approach to determine the production cost of synthetic energy carriers with a high temporal and spatial resolution on a global scale is presented and applied to Australia, New Zealand, and Germany. Hourly weather data with a spatial resolution of 0.25° x 0.25° is processed into capacity factor profiles. These capacity factor profiles, covering 11 years, are clustered into profiles including the representative weeks for each cell in the covered area using k-means clustering. The production processes of green hydrogen, ammonia, methanol as well as green crude are modeled with a generalized linear program.

The results show that low production costs can be achieved especially in Australia. Combined with large land availability, this enables large-scale synthetic energy carrier production and possible export opportunities. Hydrogen derivatives are more expensive in production, but transportation might play a significant role when deciding which synthetic energy carrier should be produced. Production costs of synthetic energy carriers in Germany are higher when compared to the model results for Australia, however, regions with favorable renewable potential might still be attractive for domestic demand.

Calculation of Synthetic Energy Carrier Production Costs with high Temporal and Geographical Resolution

Uwe Langenmayr, Manuel Ruppert
Institute for Industrial Production
Karlsruhe Institute of Technology
Germany
uwe.langenmayr@kit.edu

Abstract

While the decarbonization of the electricity sector is proceeding globally with the ongoing increase of wind and solar generation, reducing the carbon footprint of other sectors such as industry, transportation, and agriculture proves more challenging. One reason is the challenge of electrifying processes in these sectors. Here, power-to-X applications can support the transformation of these sectors by replacing conventional energy carriers with synthetic energy carriers from renewable sources.

In this work, an approach to determine the production cost of synthetic energy carriers with a high temporal and spatial resolution on a global scale is presented and applied to Australia, New Zealand, and Germany. Hourly weather data with a spatial resolution of 0.25° x 0.25° is processed into capacity factor profiles. These capacity factor profiles, covering 11 years, are clustered into profiles including the representative weeks for each cell in the covered area using k-means clustering. The production processes of green hydrogen, ammonia, methanol as well as green crude are modeled with a generalized linear program.

The results show that low production costs can be achieved especially in Australia. Combined with large land availability, this enables large-scale synthetic energy carrier production and possible export opportunities. Hydrogen derivatives are more expensive in production, but transportation might play a significant role when deciding which synthetic energy carrier should be produced. Production costs of synthetic energy carriers in Germany are higher when compared to the model results for Australia, however, regions with favorable renewable potential might still be attractive for domestic demand.

Key words: Power-to-X, linear programming, k-means clustering, synthetic energy carriers

1 Introduction and Motivation

The mitigation of climate change is a significant challenge to today's society. The transformation of the electricity sector is in full swing using renewable generation. Still, the transformation of the electricity sector is only one step towards a climate-neutral energy system. In other sectors such as industry, heating, agriculture, and transportation sector comparable carbon footprint reductions are required to meet climate targets. Especially in the industry and agricultural sectors, many processes can not be transformed by electrification. Here, conventional energy carriers are used beyond solely energy provision.

Power-to-X (PtX) processes and technologies help to use renewable electricity beyond the direct replacement of electricity generation from fossil fuel sources. With their application, several other forms of energy and synthetic energy carriers (SEC) can be generated or produced. Process heating is one major energy consumer worldwide, with a share of around 20% [16] of the global energy demand. Power-to-Heat applications allow especially low-temperature heat supply. To cover high-temperature heat demand, PtX-based energy carriers can be used and might prove a more cost-efficient solution. Power-to-Gas applications allow the production of hydrogen (H_2) and synthetic natural gas. Synthetic natural gas can be used as an energy carrier to provide high-temperature heat and close the gap in the supply of high-temperature heat. Furthermore, H_2 is required in several chemical processes like hydrocracking or hydrotreatment and enables the production of green steel via the direct reduction process. Lastly, both H_2 and synthetic natural gas further enable electricity generation via fuel cells or gas turbines.

Power-to-Liquids and Power-to-Chem applications use synthesis to convert H_2 into other SECs. The production of green crude (GC) via Fischer-Tropsch (FT) processes allows the coverage of all conventional crude oil-based products, allowing carbon-neutral fuels for transportation, plastics, waxes, and oils for the cosmetics industry. Green methanol (MeOH) produced via methanol synthesis (MeOH-Syn) can be used as a solvent or in chemical processes, and its derivatives are used in pharmaceuticals. Finally, ammonia (NH_3) from the Haber

Bosch (HB) synthesis is used to feed the world as it is the basis for fertilizer production. Altogether, PtX approaches help to replace conventional energy carriers where alternative technologies are not readily available.

2 Literature Review, Research Questions & Structure

Techno-economic analysis of PtX processes has been conducted in process simulations, energy system models or stand-alone applications. This description of existing literature in this paper focuses solely on stand-alone applications, including the integration of renewable energies via optimization methods. An extensive overview of applications and methods for PtX technologies can be found in [18].

Recent publications increasingly use optimization models to integrate volatile renewable generation into optimal PtX system configuration and production cost calculation. Linear programming models are applied to investigate the impact of volatile renewable generation on SEC production [21, 24, 27, 29]. [22] apply a mixed-integer linear program to model a superstructure with the aim of finding the cost-minimal process path to produce syngas. Open-source models have been implemented to either optimize the technical processes [2] or the electricity-based fuels production as a whole [19]. Larger scale production is optimized in [10] and [4] for the production of MeOH. [15] investigate the application of parallel methanol synthesis units regarding their ability to provide more flexibility. [30] use multi-objective optimization, including efficiency and production costs to study MeOH production.

The most similar approaches compared to our work are [9] and [26]. [9] use a baseload approach [7], which optimizes the production costs of H_2 while containing a steady H_2 supply. H_2 production costs are used as input parameters for the following techno-economic analysis of the NH_3 production. Using this approach, the actual operation of the NH_3 synthesis is not considered and therefore, its flexibility is unexploited. [26] apply their optimization model [25] in combination with weather data clustering to achieve high scalability of their model. Currently, this model is only applicable for NH_3 production and does not offer a generic formulation for different SEC.

In comparison to the above-mentioned approaches, the approach presented in this paper implements a generic PtX model, which is applicable to several SECs. The presented model can be applied globally and utilizes local data (e.g., weather data) which is available worldwide. Based on this input, weather data clustering to obtain representative weeks for each cell in the considered grid is conducted. The resulting reduced datasets allow scalability of the optimization to large areas. The main research questions of this approach are:

1. How can large-scale optimization approaches using spatial and temporal weather data with high resolution be conducted efficiently to allow a global application?
2. How can PtX approaches be modeled generically instead of the concentration on single SECs?
3. How do New Zealand and Australia perform regarding the production of SECs in comparison to Germany?

The introduction, literature review and research questions in the chapter above are followed by the description of the applied methodology in Chapter 3. Chapter 4 presents the underlying data and PtX processes considered. The results are shown in Chapter 5, followed by a summary, conclusion and critical appraisal in the last chapter.

3 Methodology

The model formulation can be divided into the processing of the weather data to obtain representative weeks of the renewable capacity factor profiles, and the optimization to minimize the production costs of the SECs.

3.1 Deriving the Representative Capacity Factor Profiles

In the first step, the weather data features are processed to obtain the capacity factor profiles of different renewable generators. Here, the open-source Python application atlite [14] is applied and combined with technical data of different renewable generators to calculate their hourly capacity factor profiles for each cell in the considered grid. This step is conducted using parallel processing in order to improve performance in handling the data with high temporal and spatial resolution.

Combining a high spatial and temporal resolution within the data results in large-scale optimization problems for each cell. To reduce input data size while maintaining the accuracy of the approach as well as possible, k-means clustering is applied to derive representative weeks for each cell in the considered grid. The resulting datasets are significantly reduced in size, while the information regarding utilization and volatility can be retained. The weekly capacity factor profiles of each generator are strung together to each other to create a vector (x_n). This is conducted for each week, creating the input matrix. A principal component analysis is used to reduce the dimension and choose the number

of clusters based on the elbow method. The reduced matrix and the number of clusters are the input of the k-means clustering algorithm, which has been applied in existing weather data clustering [13, 20, 23] and provided suitable solution. Equation (1) shows the mathematical description of k means [3].

$$\min_{b,\mu} J = \sum_{n} \sum_{k} b_{n,k} \, \|x_n - \mu_k\|^2 \tag{1}$$

The clustering will find K clusters with the cluster centers μ_k. Each vector x_n of the matrix N is assigned to one cluster. Which cluster the vector belongs to is decided via the binary variable $b_{n,k}$. The k-means clustering minimizes the total distance between each vector and the cluster center it belongs to by searching for the optimal location of the cluster center and the assignment of the vectors to the clusters. To obtain the representative weekly profile of a cluster, the vector, which is the closest to the cluster center, is chosen. The weights of the clusters are calculated by the number of weeks in the cluster divided by the total number of weeks in the matrix.

3.2 A Generic Linear Optimization Tool for PtX Processes

Type	Description
Sets	
$s \in S$	Set of commodities
$s^{MI}(k) \in MI$	Subset of commodity set representing the main input (MI) commodity of component k
$s^{MO}(k) \in MO$	Subset of commodity set representing the main output (MO) commodity of component k
$s^{F} \in FC$	Subset of commodity set representing freely available commodities
$s^{E} \in EC$	Subset of commodity set representing emittable commodities
$s^{P} \in PC$	Subset of commodity set representing purchasable commodities
$s^{M} \in SC$	Subset of commodity set representing saleable commodities
$s^{D} \in DC$	Subset of commodity set representing demanded commodities
$s^{S} \in SC$	Subset of commodity set representing storable commodities
$k \in K$	Set of conversion components
$g \in G$	Set of generator components
$c \in C$	Set of clusters
$t \in T$	Set of time steps
Variables	
x_s	Quantity of mass or energy of commodity s
$\mathrm{cap}_k, \mathrm{cap}_g, \mathrm{cap}_s$	Capacity of component
$\mathrm{soc}_{s,c,t}$	State of charge of storage component for commodity s at time t
i_k, i_g, i_s	Investment of component
Binaries	
$b_{s,c,t}^{charge}$	Charging binary for storage component of commodity s at time t
$b_{s,c,t}^{discharge}$	Discharging binary for storage component of commodity s at time t
Parameters	
$\mathrm{P}_{s,c,t}^{purchase}$	Purchase price of commodity s at time t
$\mathrm{P}_{s,c,t}^{sell}$	Selling price of commodity s at time t
W_c	Weighting of cluster c
D_s	Total demand of commodity s
$\mathrm{BU}_k^{upper}, \mathrm{BU}_k^{lower}$	Upper and lower bound of capacity utilization of conversion component k

$\mathrm{RAMP}_k^{up}, \mathrm{RAMP}_k^{down}$	Ramp-up and ramp-down rate of conversion component k
$\mathrm{CF}_{g,s,c,t}$	Capacity factor of generator g for commodity s at time t
$\eta_{k,s^{MI}(k),s}^{out}$	Conversion factor from main input main in to output s
$\eta_{k,s^{MI}(k),s}^{in}$	Conversion factor from main input main in to input s
$\eta_s^{charge}, \eta_s^{discharge}$	Charging and discharging efficiency of storage for commodity s
$\mathrm{Inv}_k, \mathrm{Inv}_g, \mathrm{Inv}_s$	Investment of components
$\mathrm{ANN}_k, \mathrm{ANN}_g, \mathrm{ANN}_s$	Annuity factor of component
$\mathrm{FOM_k}, \mathrm{FOM}_g, \mathrm{FOM}_s$	Fixed maintenance and operation of component
$\mathrm{VOM}_k, \mathrm{VOM}_g, \mathrm{VOM}_s$	Variable maintenance and operation of component
WACC	Weighted average cost of capital

The following equations describe the generic linear program to model a variety of PtX processes. The objective function includes the annualized initial investment and the maintenance of all conversion components, storage and generators.

$$\begin{aligned}\min f = &\sum_k \left(i_k(\mathrm{ANN}_k + \mathrm{FOM}_k) + \mathrm{SU}_k + \sum_c \sum_t x_{k,s^{Mo}(k),c,t}^{out} \cdot \mathrm{VOM}_k \cdot \mathrm{W}_c \right) \\ &+ \sum_{s^s} \left(i_{s^s}(\mathrm{ANN}_{s^s} + \mathrm{FOM}_{s^s}) + \sum_c \sum_t x_{s^S,c,t}^{charge} \cdot \mathrm{VOM}_{s^s} \cdot \mathrm{W}_c \right) \\ &+ \sum_g \left(i_g(\mathrm{ANN}_g + \mathrm{FOM}_g) + \sum_s \sum_c \sum_t x_{g,s,c,t}^{generation} \cdot \mathrm{VOM}_g \cdot \mathrm{W}_c \right) \\ &+ \sum_t \sum_c \left(\sum_{s^P} x_{s^P,c,t}^{purchase} \cdot \mathrm{P}_{s^P,c,t}^{purchase} - \sum_{s^M} x_{s^M,c,t}^{sell} \cdot \mathrm{P}_{s^M,c,t}^{sell} \right) \cdot \mathrm{W}_c \end{aligned} \tag{2}$$

3.2.1 Commodities

Commodities represent all mass and energy flows in the system and connect all implemented components with each other. The detailed implementation of the commodities further allows an in-depth analysis of the results to understand the interaction between all elements of the system. Balancing of all commodities during all time steps is implemented by using Equation (3).

$$\begin{aligned}&\sum_k x_{k,s,c,t}^{out} + x_{s,c,t}^{discharge} + x_{s,c,t}^{freely\ available} + x_{s,c,t}^{purchase} + \sum_g x_{g,s,c,t}^{generation} \\ &\qquad = \sum_k x_{k,s,c,t}^{in} + x_{s,c,t}^{charge} + x_{s,c,t}^{emit} + x_{s,c,t}^{sell} + x_{s,c,t}^{demand} \ \forall\ s, c, t \end{aligned} \tag{3}$$

The demand for a commodity requires the installation of sufficient capacities. Equation (4) implements the yearly produced quantity of the commodity and enables a variable hourly production.

$$\sum_c \sum_t \left(x_{s^D,c,t}^{demand} \cdot \mathrm{W}_c \right) = \mathrm{D}_{s^D} \ \forall\ s^D \tag{4}$$

Next to the demand, following equations define sources and wells which are not connected to conversion, storage or generator units. The sources and wells can only be used if specified. Otherwise, they take the value 0 for all time steps.

$$x_{s,c,t}^{freely\ available} \geq 0 \ \forall\ s^F, c, t \tag{5}$$

$$x_{s,c,t}^{purchase} \geq 0 \ \forall\ s^P, c, t \tag{6}$$

$$x_{s,c,t}^{emit} \geq 0 \ \forall\ s^E, c, t \tag{7}$$

$$x_{s,c,t}^{demand} \geq 0 \ \forall\ s^M, c, t \tag{8}$$

3.2.2 Conversion Components

Conversion components enable the system to convert commodities and allow the production of the required product. Each conversion component consists of at least one conversion, but the implementation of several inputs and outputs is possible as well. Equation (9) defines the investment of each conversion component.

$$i_k = \text{cap}_k \cdot \text{Inv}_k \; \forall \, \text{k} \tag{9}$$

As each conversion component has at least one conversion, it is characterized by at least one input and one output. One input functions as connection between conversions and capacity. It is referenced as main input $x^{in}_{k,s^{MI}(k),c,t}$. Equation (10) defines the ratio between the main input and all outputs of the same conversion component. Equation (11) uses the same approach to define the ratio between the main input and all other inputs. The parameters $\eta^{in}_{k,s^{MI}(k),s}$ and $\eta^{out}_{k,s^{MI}(k),s}$ equal zero if commodities are not output nor input of the conversion component. Equations (12) and (13) define the lower and upper bounds of the capacity utilization and the ramping ability of the conversion component.

$$x^{out}_{k,s,c,t} = x^{in}_{k,s^{MI}(k),c,t} \cdot \eta^{out}_{k,s^{MI}(k),s} \; \forall \, k,s,c,t \tag{10}$$

$$x^{in}_{k,s,c,t} = x^{in}_{k,s^{MI}(k),c,t} \cdot \eta^{in}_{k,s^{MI}(k),s} \; \forall \, k,s,c,t \tag{11}$$

$$\text{cap}_k \cdot \text{BU}^{lower}_k \leq x^{in}_{k,s^{MI}(k),c,t} \leq \text{cap}_k \cdot \text{BU}^{upper}_k \; \forall \, k,c,t \tag{12}$$

$$-\text{cap}_k \cdot \text{RAMP}^{down}_k \leq x^{in}_{k,s^{MI}(k),c,t} - x^{in}_{k,s^{MI}(k),c,t-1} \leq \text{cap}_k \cdot \text{RAMP}^{up}_k \; \forall \, k,c,t > 0 \tag{13}$$

3.2.3 Renewable Generation Units

The following Equations (14) and (15) implements the possible hourly generation, which is dependent on the hourly capacity factor of the renewable energy and the capacity of the generator. Based on the capacity, the investment of the generator is calculated. If a commodity is not generated by a generation unit, the capacity factor equals 0 for all time steps.

$$x^{generation}_{g,s,c,t} \leq \text{cap}_g \cdot \text{CF}_{g,s,c,t} \;\; \forall \, g,c,t \tag{14}$$

$$i_g = \text{cap}_g \cdot \text{Inv}_g \;\; \forall \, g \tag{15}$$

3.2.4 Storage Components

The first storage constraint defines the storage activities and their impact on the hourly state of charge (SOC). To avoid storage depletion over the considered period, the last SOC of the representative period including the last storage operation are interlinked to the first SOC of the same representative period (Equation (17)). Some storages are operated within a certain limit of the SOC (e.g., batteries to avoid degeneration). These limitations are imposed with Equation (18). Equations (19) to (21) define the storage binaries to avoid simultaneous charging and discharging. Equation (22) defines the investment of the storage component and Equation (23) prevents storage of the commodity if a storage component for this commodity does not exist.

$$\text{soc}_{s^S,c,t} = \text{soc}_{s^S,c,t-1} + x^{charge}_{s^S,c,t-1} \cdot \eta^{charge}_{s^S} - \frac{x^{discharge}_{s^S,c,t-1}}{\eta^{discharge}_{s^S}} \; \forall \, s^S,c,t > 0 \tag{16}$$

$$\text{soc}_{s^S,c,0} = \text{soc}_{s^S,c,t} + x^{charge}_{s^S,c,t} \cdot \eta^{charge}_{s^S} - \frac{x^{discharge}_{s^S,c,t}}{\eta^{discharge}_{s^S}} \; \forall \, s^S,c,t = \max(T) \tag{17}$$

$$\text{cap}_{s^S} \cdot \text{BU}^{lower}_{s^S} \leq \text{soc}_{s^S,c,t} \leq \text{cap}_{s^S} \cdot \text{BU}^{upper}_{s^S} \;\; \forall \, s^S,c,t \tag{18}$$

$$x^{charge}_{s^S,c,t} \leq b^{charge}_{s^S,c,t} \cdot \text{M} \;\; \forall \, s^S,c,t \tag{19}$$

$$x^{discharge}_{s^S,c,t} \leq b^{discharge}_{s^S,c,t} \cdot \text{M} \;\; \forall \, s^S,c,t \tag{20}$$

$$b^{charge}_{s^S,c,t} + b^{discharge}_{s^S,c,t} \leq 1 \;\; \forall \, s^S,c,t \tag{21}$$

$$i_{s^S} = \text{cap}_{s^S} \cdot \text{Inv}_{s^S} \;\; \forall \, s^S \tag{22}$$

$$\text{cap}_s = 0 \; \forall \, s \in S \cap S^s \tag{23}$$

4 Data

4.1 Weather data

In the following, the production of different SECs in Australia, New Zealand and Germany will be investigated. The weather data of each country is processed with atlite [14] using the techno-economic data in [6]. The result are hourly capacity factor profiles using the ERA 5 [12] data set. Overall, the data covers an area of 8,313,609 km² and consists of 12,481 individual cells. As the annual availability can vary significantly and therefore needs to be considered when planning PtX facilities, weather data from 2010 to 2020 is considered to include the yearly weather variation.

Table 1: Techno-economic data of renewable generators [6]

Technology	Wind	Solar
Turbine	Siemens Gamesa SG 5.0-145	-
Rotor Diameter [m]	145	-
Hub Height [m]	100	-
Specific Power [W/m²]	303	-
Efficiency [%]	-	21.5
Nominal investment [€/kW]	1040	310
Fixed O&M [%]	1.21	1
Variable O&M [€/kWh]	0.00135	0
Lifetime [years]	30	20

4.2 Power-to-X Processes

To cover a broad spectrum of SECs, the production of H_2 and its processing to MeOH, GC and NH_3 is investigated. Figure 1: Structure of the SNC production process. shows the production scheme of all SECs. The proton exchange membrane electrolysis (PEM) (3) has the advantage of reacting immediately to the volatile electricity generation and limited momentarily power availability. If the final product is MEoH, GC or NH_3, the initial output H_2 is processed further. Here, CO_2 and nitrogen (N_2) are used as additional resources. Low-temperature air separation units (ASU) (5) are able to provide CO_2 and N_2 from ambient air, allowing the production of all SECs independent from point sources. In the case of NH_3, a Haber-Bosch synthesis is implemented to convert the H_2 and N_2 into NH_3. The GC route is implemented with a reverse water gas shift (rWGS) reactor, which converts CO_2 and H_2 into synthetic gas. The synthetic gas is further processed in the FT synthesis to GC. The rWGS is assumed to be part of the synthesis for simplification. The methanol synthesis uses CO_2 directly in combination with H_2 to produce MeOH. All processes include H_2 (4) and battery storage (2). The processes are implemented with a techno-economic dataset using assumptions for characteristics in the year 2030 (Table 2, Table 3, and Table 4).

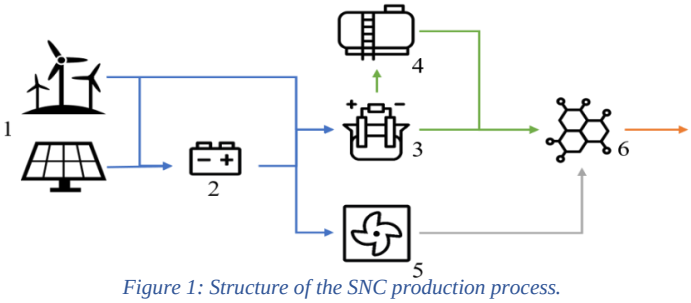

Figure 1: Structure of the SNC production process.

Table 2: Techno-economic data of PtX components

	PEM	CO_2 ASU	N_2 ASU	FT	MeOH-Syn	HB
Investment	810 [€/kW]	1656 [€/kg/h]	224 [€/kg/h]	251 [€/kW]	235 [€/kW]	574 [€/kW]
Lifetime [years]	20	20	30	25	20	30
Fixed OM [%]	3.5	4	2	6	6	2
Min. Power [%]	0	0	0	80	40	30
Max. Power [%]	100	100	100	100	100	100
Ramp-Up [%/h]	100	100	100	20	20	20
Ramp-Down [%/h]	100	100	100	20	20	20
Reference	[11]	[8]	[17]	[11]	[28]	[17]

5 Results

The maps below show the resulting H_2 production costs in Australia, New Zealand, and Germany for the year 2030. Visible by the scales next to each map, Australia achieves the lowest H_2 production costs. Additionally, low production costs are achievable in large spatial areas, allowing for the option of large-scale production. New Zealand and Germany achieve low costs only in limited geographical areas which are generally located close to the coast. In Germany, this circumstance in addition to the high industrialization, might result in the need for

additional import of H_2 and its derivatives. For New Zealand, domestic H_2 production might be sufficient due to the lower population and smaller industry sector.

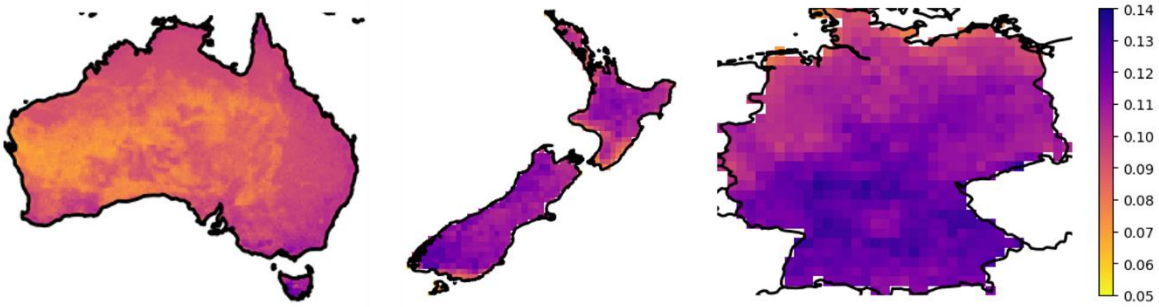

Figure 2: Production costs of H_2 [€ / kWh] in Australia, New Zealand and Germany

The comparison of the different SECs shows that H2 production results in the lowest cost in each country while all other energy carriers perform in a similar pattern for the different countries. Comparing the SEC costs from Australia to New Zealand and Germany indicates that, due to the similar production costs, transportation to New Zealand and Germany might be a viable option as ammonia, methanol as well as Fischer Tropsch crude have advantageous characteristics for long-distance transportation.

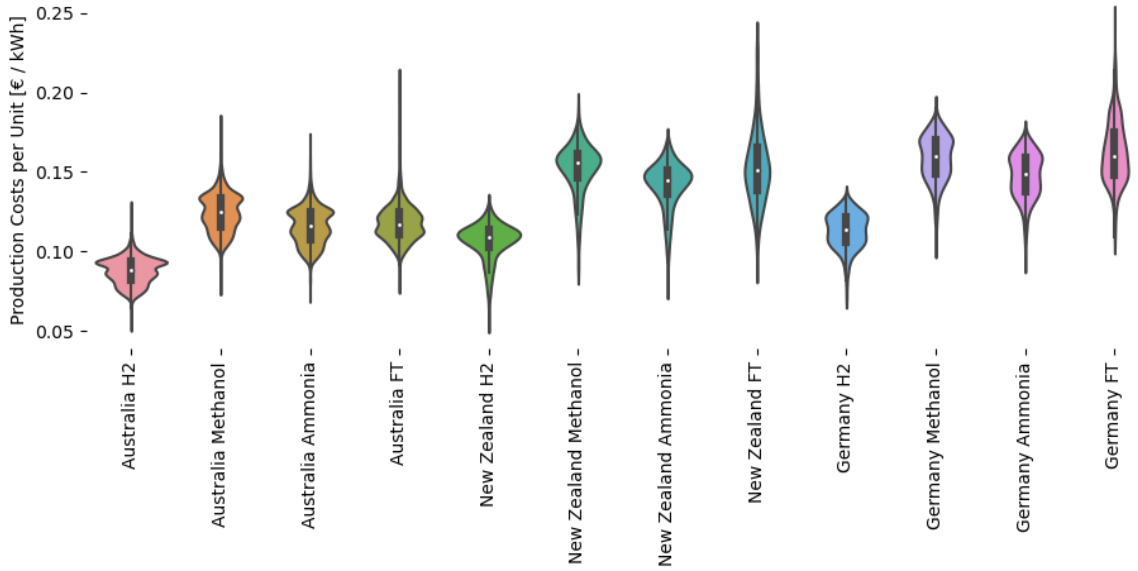

Figure 3: Production costs of different SECs at different locations.

The production costs are only one factor in the supply chain of each SEC. The transportability of the SEC is a critical aspect, especially regarding long-distance transportation. While H_2 has the lowest production costs, its energy density is low in comparison to other SECs and further steps (compression or liquefaction) are necessary before economically feasible transportation is possible. Therefore, MeOH, NH_3, and GC could be more suitable for export-destined SEC. Additionally, these SECs might be needed as chemical materials, making the synthesis indispensable.

Table 3: Techno-economic parameters of storages

Parameter	**Battery**	**H_2 Storage**
Investment [€/kW]	200	15
Lifetime [y]	15	20
Maintenance [%]	5	1
Charging Efficiency [%]	100	100
Discharging Efficiency [%]	92	100
Minimal SOC [%]	10	5
Maximal SOC [%]	90	100
Reference	[5]	[27]

6 Summary, Conclusion & Future Work

This paper proposes an approach to calculate the production costs of green hydrogen, methanol, green crude, and ammonia for large spatial areas. The weather data of Australia, New Zealand and Germany for 11 years was clustered, resulting in representative weeks. These representative weeks together with techno-economic datasets are the input of a linear optimization program using a generic formulation including multiple SEC, optimizing production cost. The results show that the production of SEC in Australia performs best. Furthermore, large areas of Australia have low production costs, resulting in potential large-scale synthetic energy carrier production.

As the size of the used input datasets requires using a clustering approach, the representative periods represent the weather conditions only imperfectly. Therefore, the result can on local production costs for an individual location can be improved using the full time-series. An analysis of the error resulting from clustering and a more detailed analysis of specific locations needs to be carried out when moving from a global model ambition towards individual site assessment. Furthermore, the linear programming approach used in this work might not be sufficient to represent the real production conditions for a specified technology of a known size. In addition, the production of SEC has not been implemented on a large scale. Therefore, current research still depends on assumptions and simplifications, as data is sparse.

The results deliver the production costs of SECs on a high spatial resolution. In future work, production quantities, based on land availability data, can be combined with the production costs to create supply curves of SEC markets. The results include optimal capacities of all components, and the dispatch of auxiliary and operating materials. Based on this data, a life-cycle assessment can be conducted to assess the environmental impact of SEC production further. Another possible future research goal is the inclusion of transportation costs of each SEC.

7 References

[1] Gorm B. Andresen, Anders A. Søndergaard, and Martin Greiner. 2015. Validation of Danish wind time series from a new global renewable energy atlas for energy system analysis. *Energy* 93, 612, 1074–1088. DOI: https://doi.org/10.1016/j.energy.2015.09.071.

[2] Mathias Berger, David Radu, Ghislain Detienne, Thierry Deschuyteneer, Aurore Richel, and Damien Ernst. 2021. Remote Renewable Hubs for Carbon-Neutral Synthetic Fuel Production. *Front. Energy Res.* 9. DOI: https://doi.org/10.3389/fenrg.2021.671279.

[3] Christopher M. Bishop. 2006. *Pattern recognition and machine learning*. Information Science and Statistics. Springer Science+Business Media LLC, New York, NY.

[4] Chao Chen and Aidong Yang. 2021. Power-to-methanol: The role of process flexibility in the integration of variable renewable energy into chemical production. *Energy Conversion and Management* 228, 6496, 113673. DOI: https://doi.org/10.1016/j.enconman.2020.113673.

[5] Wesley Cole and Frazier, Will, Augustine, Chad. 2021. *Cost Projections for Utility-Scale Battery Storage: 2021 Update* NREL/TP-6A20-79236, Golden, CO.

Table 4: Input commodities of the PtX components

	Commodity	Value	Ref
PEM	Electricity [kWh]	1.61	[11]
	Desalinated Water [kg]	0.27	
DAC	Electricity [kWh]	0.225	[8]
N_2 ASU	Electricity [kWh]	0.243	[17]
FT	Electricity [kWh]	0.069	[11]
	Hydrogen [kWh]	1.435	
	CO2 [kg]	0.249	
MeOH	Electricity [kWh]	0.101	[28]
	Hydrogen [kWh]	1.145	
	CO2 [kg]	0.25	
HB	Electricity [kWh]	0.084	[17]
	Hydrogen [kWh]	1.12	
	N2 [kg]	0.16	

[6] Energistyrelsen - Danish Energy Agency. 2022. *Technology Data. Generation of Electricity and District heating*.

[7] Mahdi Fasihi and Christian Breyer. 2020. Baseload electricity and hydrogen supply based on hybrid PV-wind power plants. *Journal of Cleaner Production* 243, 306, 118466. DOI: https://doi.org/10.1016/j.jclepro.2019.118466.

[8] Mahdi Fasihi, Olga Efimova, and Christian Breyer. 2019. Techno-economic assessment of CO2 direct air capture plants. *Journal of Cleaner Production* 224, 957–980. DOI: https://doi.org/10.1016/j.jclepro.2019.03.086.

[9] Mahdi Fasihi, Robert Weiss, Jouni Savolainen, and Christian Breyer. 2021. Global potential of green ammonia based on hybrid PV-wind

power plants. *Applied Energy* 294, 4, 116170. DOI: https://doi.org/10.1016/j.apenergy.2020.116170.

[10] Yu Gu, Danfeng Wang, Qianqian Chen, and Zhiyong Tang. 2022. Techno-economic analysis of green methanol plant with optimal design of renewable hydrogen production: A case study in China. *International Journal of Hydrogen Energy* 47, 8, 5085–5100. DOI: https://doi.org/10.1016/j.ijhydene.2021.11.148.

[11] Paul Heinzmann, Simon Glöser-Chahoud, Nicolaus Dahmen, Uwe Langenmayr, and Frank Schultmann. 2021. *Techno-ökonomische Bewertung der Produktion regenerativer synthetischer Kraftstoffe. DOI: https://doi.org/*10.5445/IR/1000140638.

[12] Hans Hersbach, Bill Bell, Paul Berrisford, Shoji Hirahara, András Horányi, Joaquín Muñoz-Sabater, Julien Nicolas, Carole Peubey, Raluca Radu, Dinand Schepers, Adrian Simmons, Cornel Soci, Saleh Abdalla, Xavier Abellan, Gianpaolo Balsamo, Peter Bechtold, Gionata Biavati, Jean Bidlot, Massimo Bonavita, Giovanna Chiara, Per Dahlgren, Dick Dee, Michail Diamantakis, Rossana Dragani, Johannes Flemming, Richard Forbes, Manuel Fuentes, Alan Geer, Leo Haimberger, Sean Healy, Robin J. Hogan, Elías Hólm, Marta Janisková, Sarah Keeley, Patrick Laloyaux, Philippe Lopez, Cristina Lupu, Gabor Radnoti, Patricia Rosnay, Iryna Rozum, Freja Vamborg, Sebastien Villaume, and Jean-Noël Thépaut. 2020. The ERA5 global reanalysis. *Q.J.R. Meteorol. Soc.* 146, 730, 1999–2049. DOI: https://doi.org/10.1002/qj.3803.

[13] Peter Hoffmann and K. H. Schlünzen. 2013. Weather Pattern Classification to Represent the Urban Heat Island in Present and Future Climate. *Journal of Applied Meteorology and Climatology* 52, 12, 2699–2714. DOI: https://doi.org/10.1175/JAMC-D-12-065.1.

[14] Fabian Hofmann, Johannes Hampp, Fabian Neumann, Tom Brown, and Jonas Hörsch. 2021. atlite: A Lightweight Python Package for Calculating Renewable Power Potentials and Time Series. *JOSS* 6, 62, 3294. DOI: https://doi.org/10.21105/joss.03294.

[15] Renxing Huang, Lixia Kang, and Yongzhong Liu. 2022. Renewable synthetic methanol system design based on modular production lines. *Renewable and Sustainable Energy Reviews* 161, 9, 112379. DOI: https://doi.org/10.1016/j.rser.2022.112379.

[16] IEA. 2018. *Clean and efficient hat for Industry* (2018). Retrieved November 4, 2022 from https://www.iea.org/commentaries/clean-and-efficient-heat-for-industry.

[17] Jussi Ikäheimo, Juha Kiviluoma, Robert Weiss, and Hannele Holttinen. 2018. Power-to-ammonia in future North European 100 % renewable power and heat system. *International Journal of Hydrogen Energy* 43, 36, 17295–17308. DOI: https://doi.org/10.1016/j.ijhydene.2018.06.121.

[18] Alper C. Ince, C. O. Colpan, Anke Hagen, and Mustafa F. Serincan. 2021. Modeling and simulation of Power-to-X systems: A review. *Fuel* 304, 121354. DOI: https://doi.org/10.1016/j.fuel.2021.121354.

[19] Philipp Kenkel, Timo Wassermann, Celina Rose, and Edwin Zondervan. 2021. A generic superstructure modeling and optimization framework on the example of bi-criteria Power-to-Methanol process design. *Computers & Chemical Engineering* 150, 107327. DOI: https://doi.org/10.1016/j.compchemeng.2021.107327.

[20] John W. Kidson. 1994. Relationship of new zealand daily and monthly weather patterns to synoptic weather types. *Int. J. Climatol.* 14, 7, 723–737. DOI: https://doi.org/10.1002/joc.3370140703.

[21] Georg Liesche, Dominik Schack, and Kai Sundmacher. 2019. The FluxMax approach for simultaneous process synthesis and heat integration: Production of hydrogen cyanide. *AIChE J* 65, 7, e16554. DOI: https://doi.org/10.1002/aic.16554.

[22] Andrea Maggi, Marcus Wenzel, and Kai Sundmacher. 2020. Mixed-Integer Linear Programming (MILP) Approach for the Synthesis of Efficient Power-to-Syngas Processes. *Front. Energy Res.* 8. DOI: https://doi.org/10.3389/fenrg.2020.00161.

[23] Robert Neal, David Fereday, Ric Crocker, and Ruth E. Comer. 2016. A flexible approach to defining weather patterns and their application in weather forecasting over Europe. *Met. Apps* 23, 3, 389–400. DOI: https://doi.org/10.1002/met.1563.

[24] Ola Osman, Sgouris Sgouridis, and Andrei Sleptchenko. 2020. Scaling the production of renewable ammonia: A techno-economic optimization applied in regions with high insolation. *Journal of Cleaner Production* 271, 1, 121627. DOI: https://doi.org/10.1016/j.jclepro.2020.121627.

[25] Nicholas Salmon and René Bañares-Alcántara. 2021. Impact of grid connectivity on cost and location of green ammonia production: Australia as a case study. *Energy Environ. Sci.* 14, 12, 6655–6671. DOI: https://doi.org/10.1039/d1ee02582a.

[26] Nicholas Salmon and René Bañares-Alcántara. 2022. A global, spatially granular techno-economic analysis of offshore green ammonia production. *Journal of Cleaner Production* 367, 3, 133045. DOI: https://doi.org/10.1016/j.jclepro.2022.133045.

[27] Dominik Schack, Liisa Rihko-Struckmann, and Kai Sundmacher. 2016. Structure optimization of power-to-chemicals (P2C) networks by linear programming for the economic utilization of renewable surplus energy. In *26th European Symposium on Computer Aided Process Engineering*, Miloš Bogataj and Zdravko Kravanja, Eds. Computer Aided Chemical Engineering, volume 38. Elsevier, Amsterdam, Netherlands, 1551–1556. DOI: https://doi.org/10.1016/B978-0-444-63428-3.50263-0.

[28] Felix Schorn, Janos L. Breuer, Remzi C. Samsun, Thorsten Schnorbus, Benedikt Heuser, Ralf Peters, and Detlef Stolten. 2021. Methanol as a renewable energy carrier: An assessment of production and transportation costs for selected global locations. *Advances in Applied Energy* 3, 12, 100050. DOI: https://doi.org/10.1016/j.adapen.2021.100050.

[29] Evan D. Sherwin. 2021. Electrofuel Synthesis from Variable Renewable Electricity: An Optimization-Based Techno-Economic Analysis. *Environmental science & technology* 55, 11, 7583–7594. DOI: https://doi.org/10.1021/acs.est.0c07955.

[30] Hanfei Zhang, Ligang Wang, Jan van herle, François Maréchal, and Umberto Desideri. 2019. Techno-Economic Optimization of CO2-to-Methanol with Solid-Oxide Electrolyzer. *Energies* 12, 19, 3742. DOI: https://doi.org/10.3390/en12193742.

Working Paper Series in Production and Energy

recent issues

No. 71 Daniel Fett, Christoph Fraunholz, Malin Lange: Provision of Frequency Containment Reserve from Residential Battery Storage Systems - A German Case Study

No. 70 Erik Jansen, Julia Schuler, Armin Ardone, Viktor Slednev, Wolf Fichtner and Marc E. Pfetsch: Global Logistics of an Iron-based Energy Network: A Case Study of Retrofitting German Coal Power Plants

No. 69 Christian Will, Florian Zimmermann, Axel Ensslen, Christoph Fraunholz, Patrick Jochem, Dogan Keles: Can electric vehicle charging be carbon neutral? Uniting smart charging and renewables

No. 68 Anthony Britto, Emil Kraft, Joris Dehler-Holland: Steelmaking Technology and Energy Prices: The Case of Germany

No. 67 Anthony Britto, Joris Dehler-Holland, Wolf Fichtner: Wealth, Consumption, and Energy-Efficiency Investments

No. 66 Martin Hain, Tobias Kargus, Hans Schermeyer, Marliese Uhrig-Homburg, Wolf Fichtner: An Electricity Price Modeling Framework for Renewable-Dominant Markets

No. 65 Martin Klarmann, Robin Pade, Wolf Fichtner, Nico Lehmann: Energy Behavior in Karlsruhe and Germany

No. 64 Florian Zimmermann, Dogan Keles: State or Market: Investments in New Nuclear Power Plants in France and Their Domestic and Crossborder Effects

No. 63 Paul Heinzmann, Simon Glöser-Chahoud, Nicolaus Dahmen, Uwe Langenmayr, Frank Schultmann: Techno-ökonomische Bewertung der Produktion regenerativer synthetischer Kraftstoffe

No. 62 Christoph Fraunholz, Kim K. Miskiw, Emil Kraft, Wolf Fichtner, Christoph Weber: On the Role of Risk Aversion and Market Design in Capacity Expansion Planning

No. 61 Zoe Mayer, Rebekka Volk, Frank Schultmann: Evaluation of Building Analysis Approaches as a Basis for the Energy Improvement of City Districts

No. 60 Marco Gehring, Franziska Winkler, Rebekka Volk, Frank Schultmann: Projektmanagementsoftware und Scheduling: Aktuelle Bestandsaufnahme von Funktionalitäten und Identifikation von Potenzialen

No. 59 Nico Lehmann, Jonathan Müller, Armin Ardone, Katharina Karner, Wolf Fichtner: Regionalität aus Sicht von Energieversorgungs- und Direktvermarktungsunternehmen – Eine qualitative Inhaltsanalyse zu Reg

Impressum

Karlsruher Institut für Technologie

Institut für Industriebetriebslehre und Industrielle Produktion (IIP)
Deutsch-Französisches Institut für Umweltforschung (DFIU)

Hertzstr. 16
D-76187 Karlsruhe

KIT – Universität des Landes Baden-Württemberg und
nationales Forschungszentrum in der Helmholtz-Gemeinschaft

Working Paper Series in Production and Energy
No. 72, September 2023

ISSN 2196-7296

www.iip.kit.edu